

# Electrochemical properties of $\text{La}_{0.8}\text{Sr}_{0.2}\text{FeO}_{3-\delta}$ – $\text{La}_{0.45}\text{Ce}_{0.55}\text{O}_{2-\delta}$ composite cathodes for intermediate temperature SOFC

Siqi Sun · Xiaodong Zhu · Yixing Yuan

Received: 18 January 2010 / Revised: 18 March 2010 / Accepted: 30 March 2010 / Published online: 20 April 2010  
© Springer-Verlag 2010

**Abstract** The electrochemical properties of  $\text{La}_{0.8}\text{Sr}_{0.2}\text{FeO}_{3-\delta}$  (LSF)– $\text{La}_{0.45}\text{Ce}_{0.55}\text{O}_{2-\delta}$  (LDC) composite cathodes coated on LSGM electrolyte were studied by electrochemical impedance spectroscopy and cathodic polarization technique. Results showed that the composite cathodes possessed superior electrochemical performance compared to that of pure LSF cathode. The cathodic overpotential of Cathode C was only 100 mV at 0.3 A cm<sup>-2</sup>, and the charge transfer resistance and the gas phase diffusion resistance were decreased to 0.105 Ω cm<sup>2</sup> and 0.257 Ω cm<sup>2</sup>, respectively at 800 °C. The improvement of the electrochemical performance is contributed to the increase of the triple-phase boundary, enlargement of the effective area for electrode reaction, and increase of the porosity of the cathode by adding LDC to the cathode material.

**Keywords** SOFC · Composite cathodes · LSF–LDC · EIS · Triple-phase boundary

## Introduction

Solid oxide fuel cells (SOFCs) are promising energy conversion devices that generate electric power through electrochemical reactions between an oxidant and a fuel [1]. Lowering the operating temperature of SOFC would bring very significant cost benefits within the scope of interconnect, manifold and sealing materials [2]. However, it is found that it leads to electrochemical performance deterioration of cathodes over time. One important approach to this problem is the application of mixed ionic and electronic conductivity cathode material such as  $\text{La}_{1-x}\text{Sr}_x\text{FeO}_{3-\delta}$  (LSF), which has high catalytic activity for oxygen reduction reaction [3–5].

Optimization of the structure and composition of composite electrodes for application in SOFC are critical. Functionally graded materials have been developed as a method of joining dissimilar materials that are usually incompatible [6, 7]. Instead of an abrupt change in composition and/or microstructure between the two materials, functionally graded materials have a graded interface at which the composition gradually changes from one material to the other [8]. The aim of this work is to apply this concept to the cathode of LaGaO<sub>3</sub>-based SOFC utilizing two materials with lanthanum-doped ceria (LDC) and strontium-doped lanthanum ferrite (LSF).

## Experimental

### Synthesis of powders

$\text{La}_{0.45}\text{Ce}_{0.55}\text{O}_{2-\delta}$  and  $\text{La}_{0.9}\text{Sr}_{0.1}\text{Ga}_{0.8}\text{Mg}_{0.2}\text{O}_{3-\delta}$  (LSGM) powders were prepared via co-precipitation method and solid-state reaction method, respectively, as in our previous

S. Sun  
The Second High School of Beijing Normal University,  
Beijing 100088, China

X. Zhu · Y. Yuan  
Center for Post-doctoral Studies of Civil Engineering,  
Harbin Institute of Technology,  
Harbin, Heilongjiang 150001, China

X. Zhu (✉) · Y. Yuan  
State Key Laboratory of Urban Water Resource and Environment,  
Harbin Institute of Technology (SKLUWRE, HIT),  
Harbin, Heilongjiang 150090, China  
e-mail: xiaodongzhu@yahoo.cn

study [9], and samples of LSF were synthesized by azeotropic distillation [10].

### Cathode fabrication

Three cathodes were screen-printed on a tape casting LSGM electrolyte substrate and then sintered at 1,250 °C for 2 h. After sintering, the resulting cathode films were  $30 \pm 1 \mu\text{m}$  thick. Table 1 and Fig. 1 show their compositions and constructions. The bottom layer for Cathode C consists of a mixture of 50 wt.% LDC and 50 wt.% LSF, the second with the composite of 30 wt.% LDC and 70 wt.% LSF, and the top layer is LSF only.

### Testing and characterization

The electrochemical impedance spectroscopy (EIS) and cathodic polarization measurements were carried out using a Princeton Applied PARSTAT 2273 by a three-electrode configuration [7]. They were performed at the open circuit voltage in the frequency range of 0.01 Hz to 100 kHz with an amplitude of ac signal of 5 mV at equilibrium potential. The impedance spectra were analyzed in terms of equivalent circuits with the ZSIMWIN software. A four-probe method was employed to measure the electronic conductivity of the composite cathode materials by a Keithley 2400 sourcemeter.

## Results and discussion

### Electronic conductivity of the composite cathode

In order to enlarge the triple-phase boundary, the electrolyte material should be mixed into the cathode material. Nevertheless, the cathodic conductivity decreased significantly with the increase of the LDC content in the cathode material. Figure 2 presents the electronic conductivities of composite cathode materials at 800 °C. Pure LSF cathode showed a high conductivity of  $115.5 \text{ S cm}^{-1}$ . The value dropped to  $11.6 \text{ S cm}^{-1}$  rapidly when the LDC content reached 50 wt.%.

### Cathodic polarization of cathodes with various structures

The cathodic overpotentials of LSF-based cathodes with different structures were measured when the half cell was

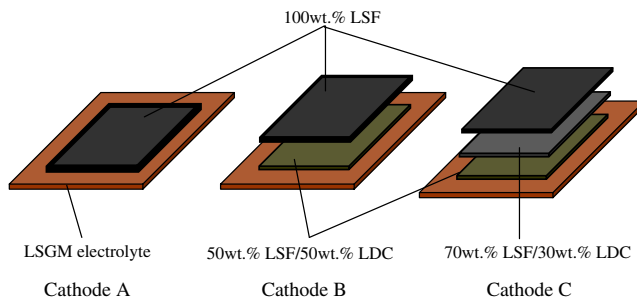


**Fig. 1** Schematic structures of Cathode A, Cathode B, and Cathode C

operated at 800 °C. Figure 3 shows the overpotentials of Cathode A, Cathode B, and Cathode C as a function of current density.

When the cathodic polarization test was carried out at 800 °C in air, Cathode C demonstrated the lowest overpotential among the cathodes. The cathodic overpotential was 100 mV at the current density of  $0.3 \text{ A cm}^{-2}$ , while the values increased to 185 and 302 mV for Cathode B and Cathode A in the same measure, respectively (Fig. 3). The reduction of the cathodic polarization was attributed to optimization of the microstructure by adding LDC to the cathode material, which would increase triple-phase boundary and enlarge the effective area for the electrode reaction.

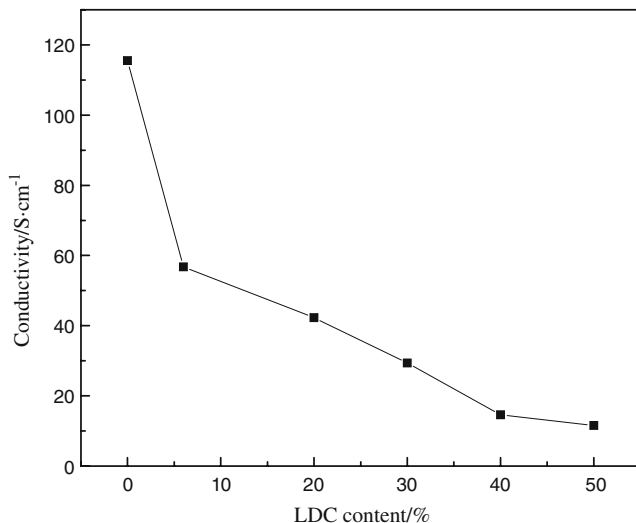
### Electrochemical impedance performances

Figure 4 shows the impedance spectra and the equivalent circuit for the half cells with various cathodes, which were measured by using a three-electrode configuration at 800 °C. The impedance spectra of cathodes were fitted using a nonlinear least squares fitting program (EQUIVCRT), and the results of these cathodes were given in Table 2.

The Nyquist plots seem to consist of two depressed semi-circles. The semicircle at the higher frequency part,  $R_{ct}$ , may correspond to charge transfer of oxygen ions at the electrolyte/electrode interface [11–13]. The low-frequency arc,  $R_c$ , is related to gas phase diffusion within the cathode [12, 13].  $L$  is the inductance, which can be attributed to the platinum current–voltage probes or the high-frequency phase shift of electrochemical equipment. The ohmic resistance ( $R_s$ ) from the electrolyte, electrodes, and the connection wires was deleted in Fig. 4 in order to compare the  $R_{ct}$  and  $R_c$  of various cathodes. The equivalent circuit consists of one  $RQ$  element. Symbol  $Q$

**Table 1** Compositions of three cathode samples

Sample	Compositions		
Cathode A		100	wt.% LSF
Cathode B	50	wt.% LSF/50	wt.% LDC
Cathode C	50	wt.% LSF/50	wt.% LDC
	70	wt.% LSF/30	wt.% LDC
		100	wt.% LSF



**Fig. 2** Conductivity of cathode material versus LDC content at 800 °C

denotes the constant phase element whose impedance,  $Z_{\text{CPE}}$ , is defined as:

$$Z_{\text{CPE}} = Y^{-1}(jw)^{-n}.$$

For  $n=1$ , the  $Q$  element reduces to an ideal capacitor with the capacitance  $Y$  and for  $n=0$  to a simple resistor with the admittance  $Y$  [14].

From Fig. 4 and Table 2, it can be seen that the charge transfer resistance ( $R_{\text{ct}}$ ) and gas phase diffusion resistance ( $R_d$ ) gradually decreased from the Cathode A, Cathode B to the Cathode C composite cathode. For the Cathode C, a  $R_{\text{ct}}$  of  $0.105 \Omega \text{ cm}^2$  and a  $R_d$  of  $0.257 \Omega \text{ cm}^2$  were obtained at open circuit voltage, and the values of Cathode B and Cathode A were  $0.240 \Omega \text{ cm}^2$  ( $R_{\text{ct}}$ ),  $0.356 \Omega \text{ cm}^2$  ( $R_d$ ),  $0.665 \Omega \text{ cm}^2$  ( $R_{\text{ct}}$ ), and  $0.386 \Omega \text{ cm}^2$  ( $R_d$ ). It can be attributed that Cathode C optimized the microstructure of electrode/electrolyte interface and increase oxygen vacan-

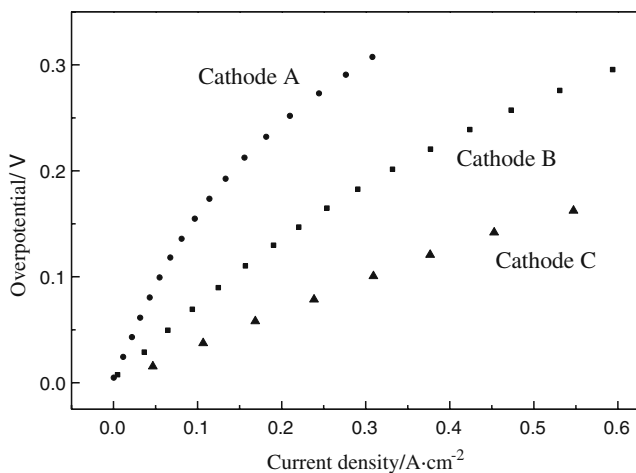


**Fig. 3** Polarization performances of cathodes with different structures

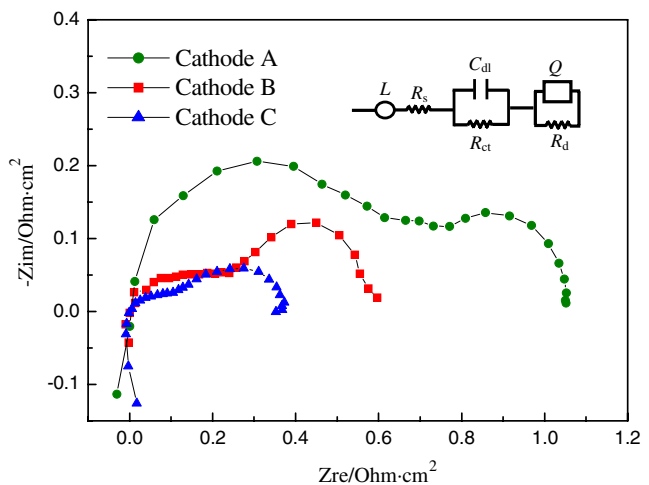


**Fig. 4** Nyquist plots and the equivalent circuit of cathodes with different structures

cies concentration at this interface by adding LDC to the cathode material. Adding appropriate excellent ionic conductor (LDC) to a mixed conducting perovskite (LSF) would increase the catalytic activity of the resultant composite cathode because additional ionic pathways are afforded for carrying reduced oxygen ions to the electrolyte [15]. Murray et al. indicate the better electrochemical performance of LSCF–GDC may be explained that the addition of GDC could extend the electrochemical reaction zone of each electrode further into the electrode and provide an easy path for ionic transport that bypasses the LSCF/YSZ interfaces [13]. Bi et al. (and Ding et al.) reported that the addition of LDC (SDC) to LSCo (LSCu) matrix effectively suppressed the growth of the LSCo (LSCu) particles grain and increased the porosity of the cathode [16, 17]. Thus in our study, the addition of LDC to LSF may increase the porosity of the inner layer because of the same reason. In the interface of electrolyte and the cathode and the cathode bulk, the addition of LDC effectively enlarged the three-phase boundary (TPB) for oxygen reduction reaction. The extended TPB resulted in a much lower polarization resistance toward oxygen reduction and higher diffusion of oxygen ions upon the addition of the ionic phase.

In our experiments, all three cathodes' films consisted of LSF, and LDC were  $30 \pm 1 \mu\text{m}$  thick. However,

**Table 2** Results of fitting EIS of different cathodes

Cathodes	$R_s/\Omega \text{ cm}^2$	$R_{\text{ct}}/\Omega \text{ cm}^2$	$R_d/\Omega \text{ cm}^2$
Cathode A	1.325	0.665	0.386
Cathode B	1.318	0.240	0.356
Cathode C	1.312	0.105	0.257

the magnitudes of ionic conductivity were substantially higher for LDC than LSF. After the ionically conducting material, LDC, was added to the LSF cathode, electrochemical reactions could occur within the electrode. So, it shortened the transport path of the oxygen ion and reduced the gas diffusion resistance for the composite cathodes. Cathode C possessed the optimal structure that exhibited the lowest gas diffusion resistance. From Fig. 4, it can be seen that the charge transfer resistance was larger than the gas phase diffusion resistance for Cathode A and the converse for Cathode C. It demonstrated that the limited step of oxygen reduction transferred from the charge transfer process to the gas phase diffusion process. Making further improvements on the electrochemical performance of LSF–LDC composite cathode could be obtained by fabricating a gradient structure, which possesses the coarse collecting current layer and the fine functional layer.

## Conclusion

The performance of the  $\text{La}_{0.8}\text{Sr}_{0.2}\text{FeO}_{3-\delta}$  and  $\text{La}_{0.45}\text{Ce}_{0.55}\text{O}_{2-\delta}$  composite cathodes was investigated. The cathodic polarization and EIS test results showed that composite cathodes possessed superior electrochemical performance compared with the pure LSF cathode. Cathode C showed the lowest cathodic overpotential magnitude 100 mV at  $0.3 \text{ A cm}^{-2}$  and the smallest charge transfer resistance as well as gas phase diffusion resistance among the LSF–LDC composite cathodes. These improvements to the electrochemical performance for LSF–LDC composite cathodes were attributed to the increase of triple-phase boundary, enlargement of

the effective area for electrode reaction and increase the porosity of the cathode.

**Acknowledgment** This project is financially supported by China Postdoctoral Science Foundation (no.20080430134 and 200902384) and Natural Scientific Research Innovation Foundation in Harbin Institute of Technology (no. HIT.NSRIF.2008.22).

## References

1. Fu CJ, Chan SH, Liu Q, Ge XM, Pasciak G (2010) Int J Hydrogen Energy 35:301
2. Singhal SC, Kendall K (2003) High temperature solid oxide fuel cells: fundamentals, design, and applications. Elsevier, Oxford
3. Matsuzaki Y, Yasuda I (2002) Solid State Ion 152:463
4. Simner S, Anderson M, Bonnett J, Stevenson J (2004) Solid State Ion 175:79
5. Simner SP, Bonnett JF, Canfield NL (2003) J Power Sources 113:1
6. Barbucci A, Bozzo R, Cerisola G, Costamagna P (2002) Electrochim Acta 47:2183
7. Zhu XD, Sun KN, Zhang NQ, Chen XB, Wu LJ, Jia DC (2007) Electrochim Commun 9:431
8. Barbucci A, Bozzo R, Cerisola G, Costamagna P (2002) Electrochim Acta 47:2183
9. Zhu XD, Sun KN, Le SR, Zhang NQ, Fu Q, Chen XB, Yuan YX (2008) Electrochim Acta 54:862
10. Zha SW, Fu QX, Lang Y (2001) Mater Lett 47:351
11. Leng YJ, Chan SH, Jiang SP, Khor KA (2004) Solid State Ion 170:9
12. Yang YL, Chen CL, Chen SY, Chu CW, Jacobson AJ (2000) J Electrochem Soc 47:4001
13. Perry ME, Sever MJ, Barnett SA (2002) Solid State Ion 148:27
14. Darja K, Panjan P, Wanzenberg E (2001) J Eur Ceram Soc 21:1861
15. Dyck CR, Yu ZB, Krstic VD (2004) Solid State Ion 171:17
16. Bi ZH, Cheng MJ, Dong YL, Wu HJ, She YC, Yi BL (2005) Solid State Ion 176:655
17. Ding XF, Cui C, Guo LC (2009) J Alloys Compd 481:845